Cavity quantum electrodynamics with quantum dots in microcavities

Gudat, J.

Chapter 8

Reflection Spectroscopy of a Quantum Dot in a Microcavity

The aim of reflection measurements performed on polarization degenerate cavities is to prove that single QDs in oxide-apertured micropillars can be used for the implementation of quantum bits. We will demonstrate a way to potentially entangle an electron spin with the photons polarization. In this way, the spin would serve as the solid state storage qubit and the photon would be used for data transfer and manipulation, as described by a hybrid quantum information system.

This chapter incorporates many ideas and techniques described in this thesis. Given the high fidelity of coupling to external modes (see Chap. 3) our spin-based quantum bits could serve as units for a scalable quantum computer either in free-space or fiber coupled [190]. Chapter 4 provides the technique to make a cavity polarization degenerate and at the same time tune the QD transition frequency into resonance with the cavity. In Chap. 5 we demonstrated how difficult and important it is to have a single QD actively interacting with one cavity. And in the previous chapter we have described schemes of how to construct such quantum computing interfaces.

8.1 Introduction

Cavity quantum electrodynamics (QED) describes the interaction between the photon and the cavity mode. Our schemes (see Chap. 7) operate deep in the weak coupling (Purcell) regime just before reaching strong coupling. In the ideal case a photon interacting on resonance with an electron spin in a cavity operating in the weak-coupling regime gets reflected. In other words,

the cavity becomes reflective in the case where light is coupled to an absorber on resonance with the cavity. In the uncoupled case, that is, the QD transition is not resonant with the cavity, the cavity is transmissive. This circumstance is illustrated in Fig. 1.19 in Chap. 1 where we plot the reflectivity as a function of the frequency of the probed light.

We will present several interesting aspects observed with reflection measurements. Unfortunately, once we could handle all the techniques to tune the QD on resonance with a polarization-degenerate cavity, our sample degraded and we had problems fabricating new ones. Therefore, we cannot present a reflection measurement where the reflection dip is close to 100%. For a non-polarization degenerate cavity a peak height visibility of 50% has been observed [55]. The samples we measured are the ones used and described in Chap. 4. (For details of the sample design and fabrication, please refer to Sect. 4.2.)

8.2 Experimental procedure

The sample is cooled to 4K in a Helium-flow cryostat. For characterization of the fundamental mode splitting and alignment procedures we pump the sample above the GaAs bandgap at 785nm with a few mW of laser power. Spectra are recorded using a single-mode fiber coupled spectrometer (resolution 0.016 nm/pixel). The laser is tightly focused on the sample by a high numerical aperture (NA) aspheric lens L_1 (focal length $f_0 = 4.02$mm, NA$= 0.6$). Before switching the setup to resonant measurements, accurate optimal alignment is crucial to observe the reflection dip. For that purpose the fundamental mode signal is maximized by tweaking the optical components including precise positioning of the piezo-driven xy-stage. Utilizing the Stark effect we tune the QD into resonance. Electrically we address the short-lived trion state of the QD. This step requires careful attention, as we have to record the optimal voltage value (on the order of 0.01V) that maximizes the QD fundamental mode emission. For the reflection measurements we switch to a tunable external cavity laser (Velocity; linewidth $<$ 300Khz) with a coarse mode-hop free tuning range of $930 - 945$nm. The mode-hop free fine tuning range is up to 80nm. The fine-frequency modulation bandwidth is 2KHz and allows fast linear sweeps (100MHz modulation bandwidth through external current supply). The fast sweeping-speed is relevant because it enables realtime measurements which simplifies further alignment procedures enormously. In order to optimize the alignment we use two photodiodes (PDs). Photodiode PD_2 measures the reflection signal while photodiode PD_1 records the reference signal that PD_2 can be normalized to. Since the reflection peak is only visible

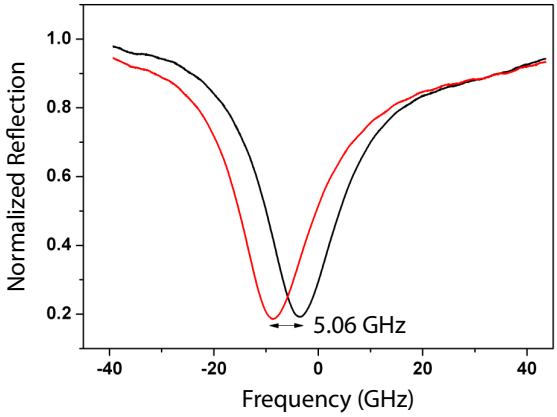

Figure 8.1: *Reflection measurements without a QD on resonance for the two orthogonally polarized fundamental modes.*

at very low powers, in the next step we replace PD_2 by a femtowatt receiver. In this configuration we can see the reflection peak in realtime and carry out further alignment optimizing the reflection peak height. In a last step, for the most sensitive measurements we replace both PDs by avalanche photodiodes (APDs). For accurate power measurements we used a power meter and optical density (OD) filters.

8.3 Experimental results

In Chap. 4 Sect. 4.4 we demonstrated the tuning of a QD transition to a degenerate microcavity resonance. For the same cavity Fig. 8.1 shows the two reflection dips for the two orthogonally polarized fundamental modes with a separation of about 5GHz and a coupling efficiency of around 80%. However, for a sufficiently degenerate cavity we would need a splitting $\sim$ 2GHz.

Nevertheless, coupling the light to one polarization of the cavity we could theoretically expect a peak height of up to 50%. Spectrally, the QD emission maximized the fundamental mode signal when applying a bias of $1.13V$. Figure 8.2 depicts a typical result of our search for QD related peaks in the spectrally-broad reflections dips. It shows a reflection peak which only has a height of around 5%.

A possible explanation for the small peak height could be that the QD is spatially located too far away from the cavity center. To support this hypothesis, we spectrally detune the QD from the fundamental mode by applying a

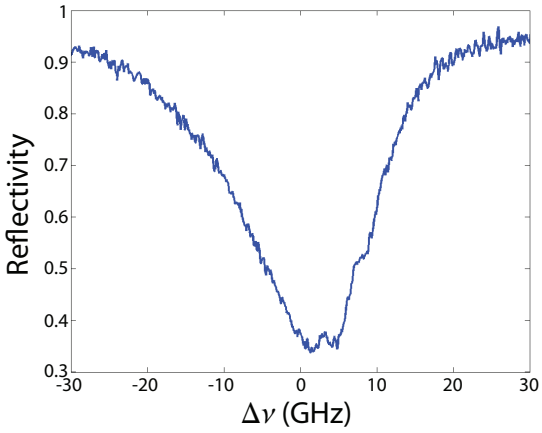

Figure 8.2: *Reflection measurement on a degenerate cavity with a QD tuned into resonance. The height of the reflection peak at $\nu = 3GHz$ is very small around 5%. This is the same cavity investigated and shown in Fig. 4.11 in Chap. 4.*

bias of 1.204V instead of 1.13V and perform a spatial scan. The $10 \times 10\mu$m scan is shown in Fig. 8.3 for two different wavelengths. The peak of the QD emission (a) is visible at 943.10nm while the fundamental mode (b) is observed at 943.13nm. The QD emission is clearly visible in (b) spatially located away from the fundamental mode emission center. Gaussian fitting of both the fundamental mode and the QD allows one to compute their relative separation to be around 4.3μm. For our cavities with an approximate beam waist of $w_0 = 1.5\mu$m it is crucial to have a QD positioned within 1μm from the cavity center. Higher reflection peaks (up to 30%) have been measured by us on numerous other cavities and are presented as part of the following measurements.

When tuning the QD into resonance, spectrally it is very easy to observe how QDs maximize the fundamental mode signal. Reflection measurements in comparison allow one to monitor the effect of the Stark tuning more precisely. In Fig. 8.4 a series of reflection measurements for increased voltage values in very small steps on the order of $0.0025V$ are shown. When setting up the experiment, finding the correct voltage value can be very critical. For the presented example a voltage range of $\Delta V = 0.03V$ already tunes the QD completely out of resonance.

The pump power dependance has a few interesting aspects. Literature describes that with increasing pump-power the height of the peak in the dip decreases nonlinearly [54, 55]. This effect has been confirmed [114] and could

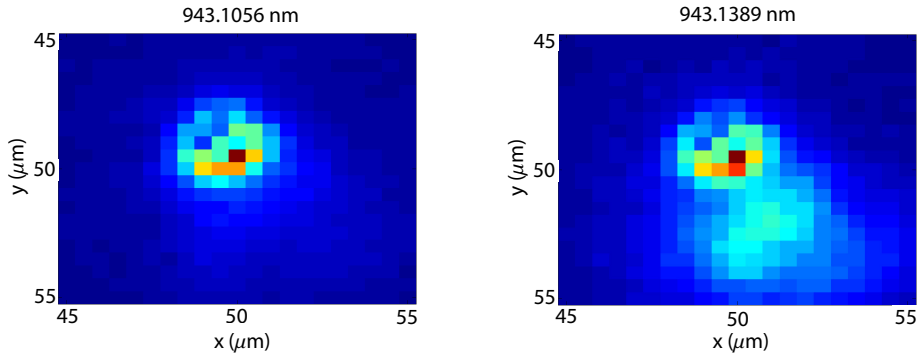

(a) Quantum dot (b) Fundamental mode

Figure 8.3: *Spatial scan for the same cavity as presented in Fig. 8.2 with a detuned QD by applying a bias of* $1.204\,V$. *QD (a) peak appears at lower wavelength (*$943.10nm$*) than the fundamental mode peak (b) at* $943.13nm$. *In (b) both the QD and the fundamental mode are visible as the QD still partially couples to the fundamental mode. The distance between the QD and the emission center of the fundamental mode is* $4.3\mu m$.

also be observed in our measurements. This reflection peak decrease for increased pump powers is illustrated in Fig. 8.5 for three different pump-powers, (a) pump 7.5pW, (b) pump 75pW and (c) pump 375pW.

From the Jaynes-Cummings Hamiltonian using the input-output formalism for weak probing of a symmetric cavity, the reflection spectrum can be described by [54]:

$$R(\omega) = \left| 1 - \frac{\kappa(\gamma - i(\omega - \omega_{QD}))}{(\gamma - i(\omega - \omega_{QD}))(\kappa - i(\omega - \omega_{cavity})) + g^2} \right|^2, \tag{8.1}$$

where g is the dipole-constant, κ the cavity decay rate, and γ the dipole decay rate. ω_{QD} and ω_{cavity} are the resonance frequencies of the QD and the cavity, respectively. We fit this formula to the data to retrieve the height of the peaks. This cavity was non-polarization degenerate which means we do not pump a single spin but rather have to average over a coupled ($g \neq 0$) and a non-coupled ($g = 0$) case. Additionally we take the offset of our non-perfectly mode matching coupled system into account.

$$R_{fit}(\omega) = \frac{R(\omega, g \neq 0) + R(\omega, g = 0)}{2} + \text{offset} \tag{8.2}$$

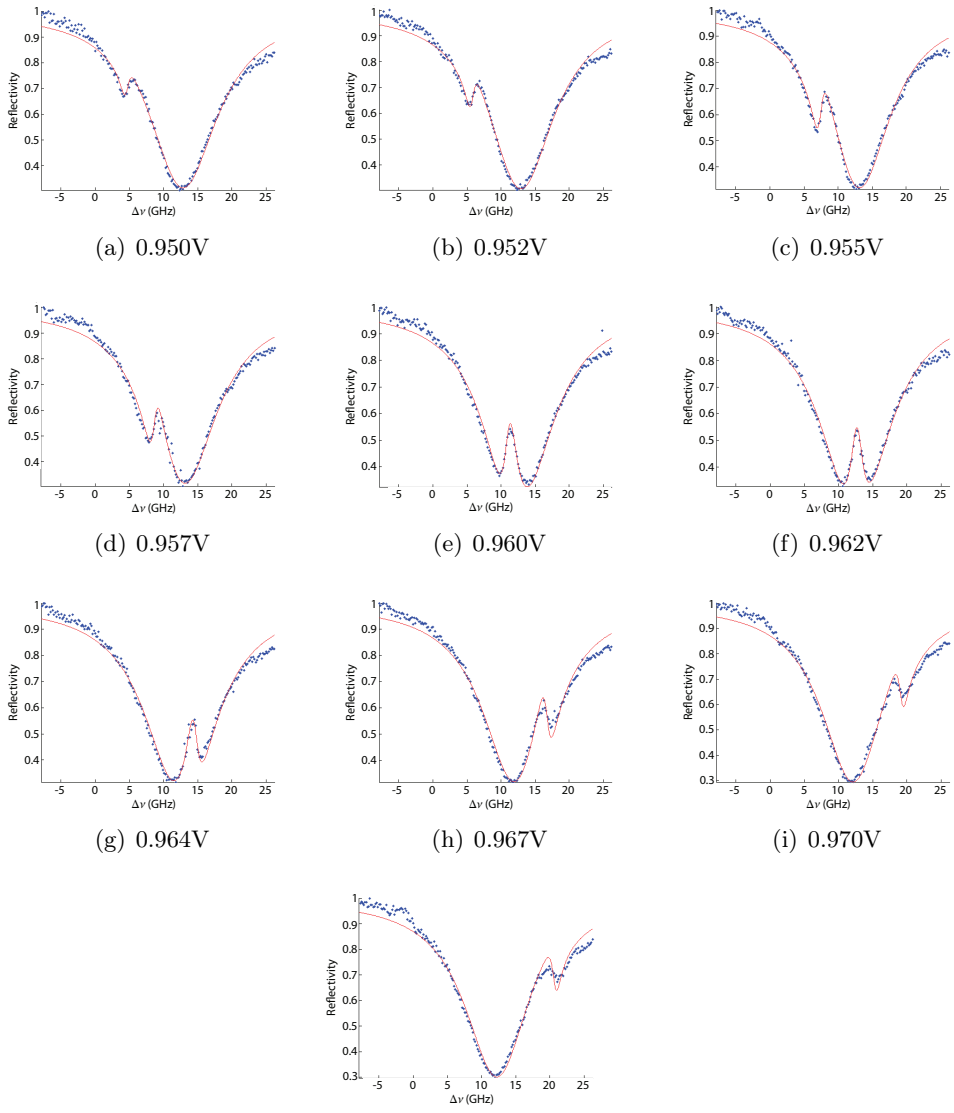

(a) 0.950V (b) 0.952V (c) 0.955V

(d) 0.957V (e) 0.960V (f) 0.962V

(g) 0.964V (h) 0.967V (i) 0.970V

(j) 0.972V

Figure 8.4: *Tuning of reflection dip.*

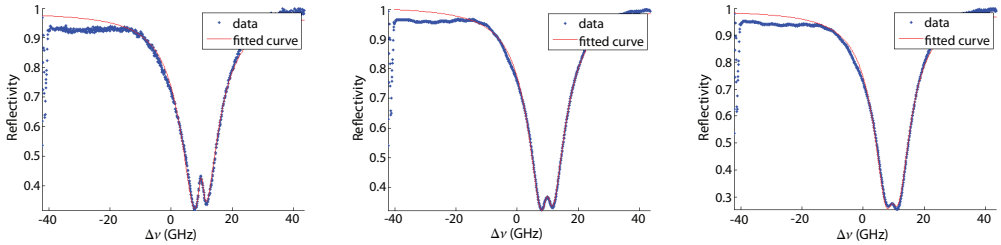

(a) 7.5pW (b) 75pW (c) 375pW

Figure 8.5: *Reflection peak decrease for increased pumped powers. Pumping with (a) 7.5pW, (b) 75pW and (c) 375pW.*

The resulting height of the peaks is with respect to an empty cavity without a reflection peak with the same coupling efficiency. The effect of the *reflection peak nonlinearity* is shown in Fig. 8.6 for 16 measurements. The curve is fitted to the predicted visibility $V(P)$ as a function of power P [54]:

$$V(P) = \frac{V_0}{(1 + P/P_{critical})^2}, \tag{8.3}$$

where $P_{critical}$ is the critical power at which the visibility reduces to 25%. We obtain a visibility of $V_0 = 0.134$ and a critical power value of $P_{critical} = 271\text{pW}$. The latter value corresponds to about 1.27×10^9 photons per second reaching the cavity. Since the lifetime of the cavity is about $100 - 200\text{ps}$ about one fifth to one quarter of the photons interact with the cavity per lifetime.

The reflection peak nonlinearity may be explained by considering a few single photons reaching the cavity. The first photon interacting with the cavity gets absorbed and causes the QD to jump from its ground state to its excited state. For as long as the QD stays in the excited state none of the other incoming photons can interact with the QD and get reflected. For those photons the cavity stays transmissive.

Reflection spectroscopy with the proposed system is experimentally the most complicated of all the measurements performed in this thesis. It comprises of many different techniques. Unfortunately we cannot present a fully polarization-degenerate cavity with which we could have performed all the experiments shown or described. Nevertheless, we present a reflection measurement with a fully polarization-degenerate cavity in Fig. 8.7. After burning 27 holes we could reduce the fundamental mode splitting from 50GHz to 0.2GHz.

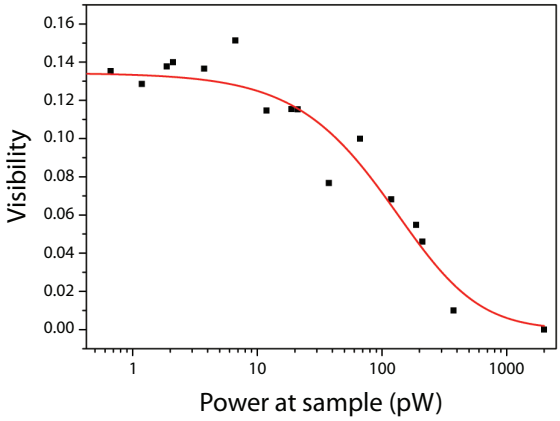

Figure 8.6: *Power dependence of the peak height.*

Unfortunately we had no QD available that could couple resonantly with the cavity.

8.4 Conclusion and discussion

Experimentally we have demonstrated the complexity of reflection spectroscopy measurements of single QDs in microcavities. All techniques developed in this thesis are crucial for demonstrating a quantum bit implementation with a single QD in an oxide-apertured micropillar. We demonstrated that we mastered all the requirements separately but could not yet perform a final measurement on a polarization-degenerate cavity with a single QD tuned into resonance spatially located close enough to the cavity center for optimal performance. We have shown that reflection spectroscopy is a method to gain more insight into the micropillars potentially serving as qubits. In particular, we did observe the reflection peak nonlinearity in accordance with literature.

Worried about the degradation of our samples, especially due to the hole burning technique, we systematically monitored their IV-curves. Multiple cooling cycles and applying electrical fields via the diode-structure (and by that causing currents heating the sample) over long times (e.g. during spatial scans) are also potential sources of degeneration. Degradation appeared sudden. The samples were useable for a long time (around one year) and degraded almost over night for no obvious reason.

In conclusion, we have come a very long way in designing, fabricating and fine-tuning micropillar cavities with embedded charge tunable QDs. We

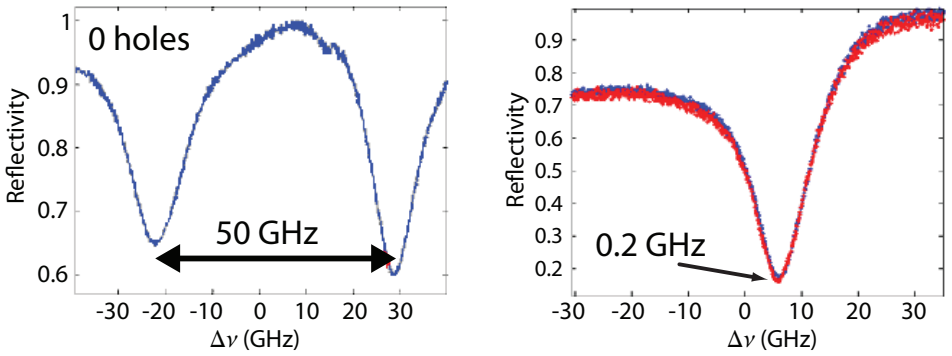

(a) Initial splitting of 50GHz

(b) Polarization degenerate cavity with splitting of 0.2GHz

Figure 8.7: *Reflection measurements of a polarization-degenerate cavity. By burning 27 holes, the initial splitting of the fundamental mode showing 2 dips separated by* $50\,GHz$ *(a) is reduced to a minimal splitting of* $0.2\,GHz$ *(b).*

have obtained good experimental results on single QD single mode interactions. Topics for further improvements are to have all demonstrated tuning methods, such as active positioning, charge tuning, Stark shift tuning, and polarization tuning, working simultaneously. This challenge is being taken on by my successors in the group of D. Bouwmeester.